

GENERATION OF FEMTOSECOND ELECTRON BUNCHES AND HARD-X-RAYS BY ULTRA-INTENSE LASER WAKE FIELD ACCELERATION IN A GAS JET

M. Uesaka, T. Hosokai, K. Kinoshita¹⁾, A. Zhidkov¹⁾
 Nuclear Engineering Research Laboratory, University of Tokyo
¹⁾ National Institute of Radiological Sciences, Japan

Abstract

Femtosecond electron beams and hard x-rays with $\lambda \sim 0.1$ nm may find various applications in biology, chemistry, and microelectronics giving a new time-scale probe analysis. Such short electron beams can be produced in the wake field acceleration by short relativistically intense laser pulses and then Thomson scattering of a second laser pulse can serve for efficient generation of very short x-rays with use of such electron beams.

INTRODUCTION

We study experimentally with 12 TW, 50 fs Ti-sapphire laser set-up and numerically through a multidimensional particle-in-cell simulation two mechanisms of generation of femtosecond electron bunches in gas jet suitable for efficient Thomson scattering. The first is the LWFA of electrons injected due to wave-breaking on a shock-wave produced by a laser prepulse in a He gas-jet. This mechanism allows us to produce a narrow-coned electron bunch with duration around 40 fs. Results of measurements agree well with two-dimensional hydrodynamics and particle-in-cell simulations. Such a beam can scatter up to 10^9 photons per pulse in 1° cone. Spectrum of scattered light is discussed. Because of large energy spread of electrons in a bunch, the x-ray spectrum is broad. To overcome this problem another mechanism, self-injection of plasma electrons, is proposed and studied numerically. The self-injection of plasma electrons which have been accelerated to relativistic energies by a laser pulse moving with a group velocity less than the speed of light appears when $a_0 \geq \sqrt{2}(\omega / \omega_{pl})^{2/3}$ where a_0 is normalized laser field. In contrast to the injection due to wave-breaking processes, self-injection allows extraction of a beam-quality bunch of energetic electrons. This injection is also expected to be useful in generation of very short pulse, ~ 10 fs, electron beams with the charge ~ 100 pC. The diameter of such a beam in a gas jet after acceleration is only 5-10 μm that makes possible the production of high-brightness hard-x-rays with few percent energy spread by using contrary propagating laser pulses. The efficiency and spectrum of such x-rays are calculated and discussed.

EXPERIMENTAL SET-UP

An intense and ultra-short laser pulse has been focused on helium gas (see Fig. 1). In order to form a spatially localized gas column, to suppress the transverse expansion into vacuum due to the thermal and fluid motion of the injected gas, a supersonic pulsed gas

injection has been used as a target. The pulsed gas jet has been produced by a device consist of an axially symmetric Laval nozzle and a solenoid fast pulse valve. The nozzle was designed to provide the Mach number $M=4.2$ at the exit of the nozzle. It has a 2.0 mm inner diameter at the exit. The typical experimental set-up is shown in Fig.1. The nozzle with the pulse valve

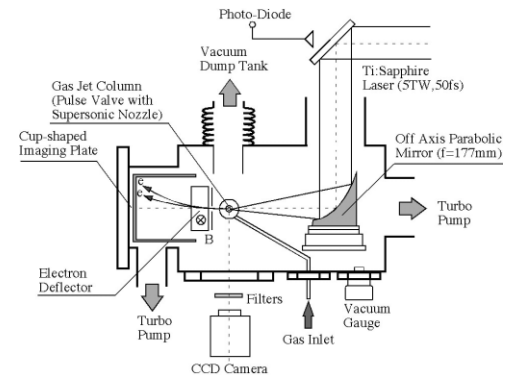


Fig.1 Experimental set-up .

was placed inside the vacuum chamber. The pulse valve was driven for 5 ms a shot at a repetition rate of 0.2 Hz. The stagnation pressure of the valve is varied from 5 to 20 atm. With these pressures the density at the exit of the nozzle ranged from 7×10^{18} to $3 \times 10^{19} \text{cm}^{-3}$.

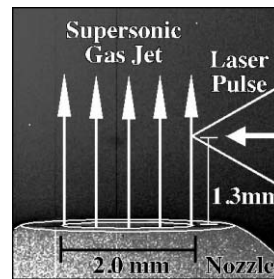


Fig. 2 Supersonic gas jet and laser focus position.

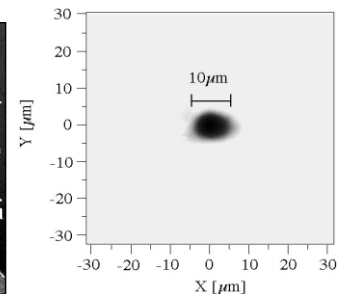


Fig. 3 Image of the laser focal spot at the target.

The 12TW Ti:Sapphire laser system based on CPA technique generated up to 600 mJ, 50 fs laser pulses at fundamental wavelength of 790 nm with 10 Hz repetition rate. The laser power at the target in the vacuum chamber was up to 5TW. As shown in Fig.2, the p-polarized laser pulse with diameter of 50 mm was delivered into the vacuum chamber through a vacuum laser transport line and was focused on the front edge of helium gas jet column at the height of 1.3 mm from nozzle exit with an $f/3.5$ off-axis parabolic mirror (OAP). Fig. 2 gives side-

view of the interaction region obtained by the CCD camera, and illustrates the gas jet and the focus point. Fig. 3 shows a typical image of a laser focal spot at the target position. The spot size was $7.5 \mu\text{m}$ in full width at $1/e^2$ of maximum. The maximum laser intensity on the target was estimated as 10^{19} W/cm^2 so that the laser parameter a_0 exceeded 2.0.

SELF-INJECTION IN LWFA

Injection of electrons for their further acceleration is a crucial part of LWFA [1]. Usually for LWFA, the injection of a high quality electron beam from a RF accelerator is assumed [2]. In other schemes, two or several laser pulses are employed for the injection [3]. Such schemes require highly precise synchronization between the wake-field and the injection. Moreover, though the LWFA, particularly, allows the production of an ultra-short electron bunch (~ 10 fs), which is necessary for probe-analysis of matter [4], the schemes based on an external injection hardly be applied for this. Another way for electron injection exploits an injection produced by the laser pulse itself, so-called 'self-injection'. A short laser pulse consists of a short (~ 50 - 100 fs) intense part, main pulse, and a long (~ 2 - 10 ns) pedestal which is usually called as a prepulse and a post pulse. The intensity of the prepulse varies from 10^{-5} down to 10^{-7} from that of the main pulse. Self-injection schemes can exploit both parts of the laser pulse. The prepulse can be used to form a proper condition for the wave-breaking injection of electrons to the wake-field while the main pulse can produce injection by itself due to relativistic effects.

If the Raleigh length, L_R , for the laser pulse is short enough, the prepulse can form a cavity with a shock wave in the front of laser propagation. In contrast to the plasma channel produced by long Raleigh length laser beam [5], the length of the cavity is determined by this small L_R , because the energy is deposited in the plasma mostly near the focus point $x=0$ as $W(x) \sim 1/(1+(x/L_R)^2)$. For low intensity laser pulse, the electron temperature, T_e , can be estimated via the collisional absorption mechanism, $dT_e/dt = \Delta\epsilon \nu_{ei}(1\text{eV})/T_e^{3/2}$, where $\Delta\epsilon = 2\pi e^2 I/m\omega^2$ the energy acquired by an electron in a collision; ν_{ei} the frequency of electron-ion collisions. For intensity $I=10^{13} \text{ W/cm}^2$ and ion density $N_i=3 \times 10^{18} \text{ cm}^{-3}$ (in the cavity) and pulse duration $\tau=2 \text{ ns}$, $T_e=150 \text{ eV}$. If $X=C_s \tau > L_R$, where C_s the ion sound speed, a shock wave can be formed in the plasma. If the shock wave relaxation depth $\Delta x \sim (M/m)^{1/2} l_i$ (M is the ion mass, l_i the ion free path) less than the plasma wave wavelength l_{pl} , the strong wave-breaking of wake-field produced by the main pulse there can be a good source of injection. For temperature $T_e \sim 150 \text{ eV}$ in a He gas-jet, the ion sound speed is $C_s \sim 5 \times 10^6 \text{ cm/s}$ and $X \sim 100 \mu\text{m}$ so that the effect appear for the laser pulse with the Raleigh $L_R < 100 \mu\text{m}$. The shock wave can be generated in get with $\omega_{pl} l_i (M/m)^{1/2} / 2\pi c > 1$ that gives $N_i > 5 \times 10^{18} \text{ cm}^{-3}$. The density gradient at the shock wave is steep and effective wave-breaking is appeared [6].

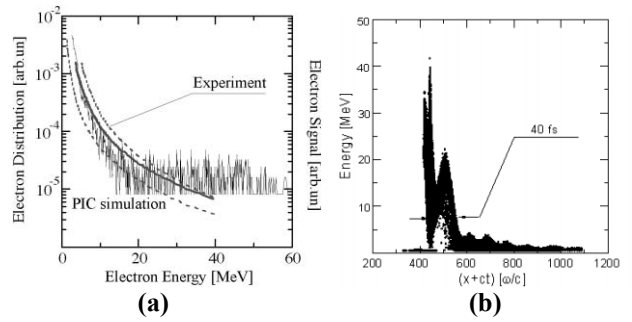


Fig.4 The measured and calculated time-integrated (a) and spatial (b) energy distribution of electrons in the bunch for the laser power of 4TW.

In order to obtain the energy distributions of the electrons, a magnetic electron deflector was set in the laser axis behind the jet (as shown in Fig.1). The bottom plate of the cup is used as an electron detector. The magnetic field between the magnets is mapped out with a Hall probe and the maximum field strength reaches 300 mT. That has an entrance aperture of 2.0 mm with an acceptance solid angle of 1 msr. With this set-up, the energy distribution of the ejected electrons up to 40 MeV can be detected. Measured distribution of narrow-coned electrons is shown in Fig.4. The distribution agree well with that obtained in 2D particle-in-cell calculation. This energy distribution is Maxwell-like with the effective temperature $T_h \sim 10 \text{ MeV}$, and the maximal energy we observed is 40 MeV. The electrons with energy from 10 to 40 MeV constitute a bunch with duration of 40 fs in PIC simulation. The calculated charge of electron bunch is 0.7 nC/1J. In Fig.4b the spatial distribution of accelerated electrons obtained from PIC simulation shows the bunch duration is 40 fs!

The wave-breaking is initially a stochastic process that provokes rapid randomization in energy of accelerated electrons. This makes such kind of injection sometimes inefficient and usually very sensitive to plasma parameter changes. A mechanism of electron injection originating from the relativistic character of the laser-plasma interaction can be applied to improve the energy spread of accelerated electrons.

Along with the common wake-field, a relativistically intense laser pulse moving in an under-dense plasma with group velocity less than the light speed generates additional electrostatic wave, which has a group velocity close to the group velocity of the laser pulse from the linear theory. This wave comes from electrons temporally trapped and accelerated directly by the laser pulse forming a bunch at the front of the laser pulse. This bunching of electrons creates a potential difference, potential cavity [6], behind the laser pulse due to the evacuation of electrons. The number of electrons in this bunch is limited by repulsion; the repealed electrons are accelerated to energy equal the potential difference in the cavity and, thus, can be efficiently injected for further acceleration if proper matching condition occurs. However this injection, which can be considered as a self-

injection, contends with injection after wave-breaking. At low plasma density, the self-injection produces efficient acceleration with a low energy spread while at high density, wave-breaking dominates producing a Maxwellian distribution of energetic electrons with an effective temperature. Propagating in under-dense plasma with the group velocity, v_g , an intense laser pulse can accelerate plasma electrons, which are in the rest at the beginning, up to the energy $\varepsilon_{e_{\max}} = mc^2 a_0^2 / 2$, where $a_0 = eE/mc\omega$ with E the laser electric field, and ω the laser frequency. If the velocity of such electrons exceeds the group velocity of the laser pulse, these electrons can be trapped and move with the pulse forming an electrostatic wave. The matching condition can be written in the following form, $\gamma_{e_{\max}} = a_0^2/2 = \gamma_g = 1/(1-v_g^2/c^2)^{1/2} \sim \omega\gamma_e^{1/2}/\omega_{pi}$ where ω_{pi} is the plasma frequency and $\tilde{\gamma}_e \sim \sqrt{1+a_0^2/2}$ is the electron quiver energy. The potential difference, $\Delta\phi$, produced by electrons directly accelerated by the laser at the front of the pulse cannot exceed the ponderomotive potential $mc^2 a_0^2/2$. As a result, the length of the cavity behind the laser pulse is $d = \lambda_0 a_0/2\pi$. At this distance behind the laser pulse the reaped electrons acquire energy $\varepsilon = |\Delta\phi|$ and, moving with the group velocity, are further accelerated in the cavity. For mono-energetic acceleration, d must exceed the pulse length $c\tau$, where τ is the pulse duration. The maximal energy finally acquired by such an electron is $E_{\max} = (a_0/2\pi)E_{\max}^{WF}$, where E_{\max}^{WF} is the corresponding maximal energy in acceleration by longitudinal plasma wave.

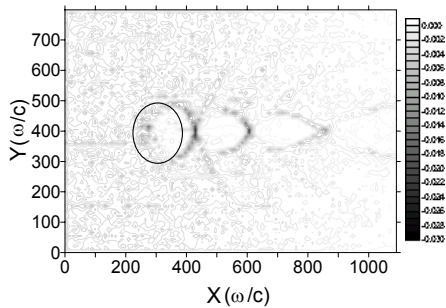


Fig.5 The spatial distribution of normalized density of electrons in the gas-jet of density, $N_e = 10^{19} \text{ cm}^{-3}$, at $\omega t = 4000$ for $I = 10^{20} \text{ W/cm}^2$; $X = x + ct$

Results of 2D simulation displaying the formation of the electrostatic wave are shown in Fig.5. One can see a clear cavity structure in electron density after the pulse propagates 0.5 mm in the plasma though there is no wave-breaking of the plasma wave. The transverse size of the first bunch in the rear of the first cavity is about $10 \mu\text{m}$. The energy distribution of electrons in the bunch after the pulse past 1 mm and 2 mm in the plasma are shown in Fig.6. The both distributions have a peak that corresponds to electrons accelerated after the self-injection. The energy spread is 5% in both cases although energy spread in the pedestal increases considerably. Formal calculation of the emittance in the bunch gives that of $0.1 \pi \text{ mm mrad}$

at total charge $Q \sim 100 \text{ pC}$.

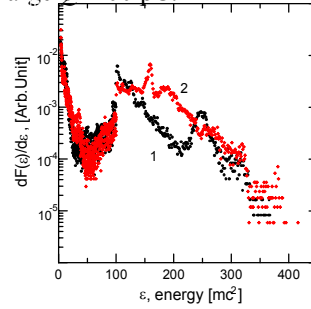


Fig.6 Electron energy distribution in 2D PIC simulation; $I = 10^{20} \text{ W/cm}^2$, $\tau = 20 \text{ fs}$, $\omega t = 6000$ (a) $\omega t = 12000$ (b) at the plasma density $N_e = 10^{19} \text{ cm}^{-3}$

THOMSON SCATTERING

Moving through the laser pulse, a relativistic electron transforms the laser light to X-rays. The total number of photons produced by an electron strongly depends on the intensity of the scattered light and can be found from simple equation, $dn/dt = \sigma I/h\omega$, where $\sigma \sim \pi r_e^2 = \pi e^4/(mc^2)^2$ electron cross-section, n the number of x-ray photons. For the laser pulse with total energy 1 J, $\lambda \sim 1 \mu\text{m}$, and focus spot $\sim 10 \mu\text{m}$ - $W = 1 \text{ MJ/cm}^2$ that gives $n \sim 2-3$. Electron bunch, 40 fs, 100 pC, can produced 10 keV x-rays in 1° with 10^9 photons and duration $\sim 30 \text{ fs}$. A typical spectrum of scattered signal is given in Fig. 7 for $a_0 = 2$ [2]

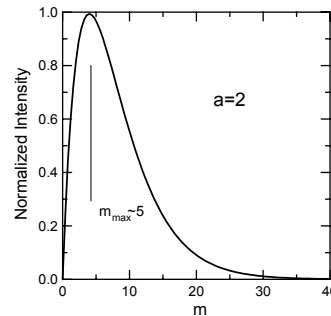


Fig. 7 Typical spectrum of scattered x-rays [2]. The maximum frequency is $\omega \sim m\omega_0 8\gamma_0^2/(1+a_0^2)$ with γ_0 the energy of accelerated electrons.

REFERENCES

- [1] T. Tajima and J. Dawson, Phys. Rev. Lett., **43**, 267 (1979); K. Nakajima et al., Phys. Rev. Lett. **74**, 4428 (1995); F. Dorchies et al., Phys. Plasmas **6**, 2903 (1999).
- [2] D. Umstadter et al., Science **273**, 472 (1996); Phys. Rev. Lett. **76**, 2073 (1996); Phys. Rev. Lett., **90**, 055002 (2003)
- [3] E. Esarey, R.F. Hubbard, W.P. Leemans, A. Ting, and P. Sprangle, Phys. Rev. Lett. **79**, 2682 (1997); IEEE Trans. Plasma Sci., **24**, 252 (1996)
- [4] M. Uesaka, et al, Phys. Rev E **50**, 3068 (1994); Radiation Physics and Chem. **60**, 303(2001); Nucl. Instr. Meth. Phys. Res. A **455**, 148 (2000); Phys. Rev. ST Accel. Beams **5**, 041301 (2002)
- [5] V. Malka, et al., Phys. Plasmas **8**, 2605 (2001); Science, **298**, 1600 (2002); Phys. Plasmas **6**, 2903 (1999); Phys. Plasmas **7**, 3009 (2000)
- [6] T. Hosokai, et al., Phys. Rev. E **67**, 036407 (2003); A. Zhidkov, et al, Phys. Rev. Lett. (in press)